Glucose-1,6-bisphosphate, a key metabolic regulator, is synthesized by a distinct family of α-phosphohexomutases widely distributed in prokaryotes

Niels Neumann[1,2], Simon Friz[1,2] and Karl Forchhammer[1,2*]

[1] Interfaculty Institute of Microbiology and Infection Medicine, University of Tübingen, Auf der Morgenstelle 28, 72076 Tübingen, Germany

[2] Cluster of Excellence: EXC 2124: Controlling Microbes to Fight Infection, Tübingen, Germany

* For correspondence: karl.forchhammer@uni-tuebingen.de

Abstract

The reactions of α-D-phosphohexomutases (αPHM) are ubiquitous, key to primary metabolism and essential for several processes in all domains of life. The functionality of these enzymes relies on an initial auto-phosphorylation step which requires the presence of α-D-glucose-1,6-bisphosphate (Glc-1,6-BP). While well investigated in vertebrates, the origin of this activator compound in bacteria is unknown. Here we show that the Slr1334 protein from the unicellular cyanobacterium *Synechocysitis* sp. PCC 6803 is a Glc-1,6-BP-synthase. Biochemical analysis revealed that Slr1334 efficiently converts fructose-1,6-bisphosphate (Frc-1,6-BP) and α-D-glucose-1-phosphate/α-D-glucose-6-phosphate into Glc-1,6-BP and also catalyzes the reverse reaction. As inferred from phylogenetic analysis, the *slr1334* product belongs to a primordial subfamily of αPHMs that is present especially in deeply branching bacteria and also includes human commensals and pathogens. Remarkably, the homologue of Slr1334 in the human gut bacterium *Bacteroides salyersiae* catalyzes the same reaction, suggesting a conserved and essential role for the members of this αPHM subfamily.

Key words:

Phosphoglucomutase, glucose-1,6-bisphosphate, fructose-1,6-bisphosphate, glycolysis, carbon metabolism

31 # Introduction

32 The α-D-phosphohexomutase (αPHM) superfamily is ubiquitous and found in all domains of
33 life. All known members of this superfamily catalyze a reversible intramolecular phosphoryl
34 transfer on their phosphosugar substrates. This reaction requires a bound metal ion (usually
35 Mg^{2+}) together with a conserved phosphorylated seryl residue in the active site and proceeds
36 via a bis-phosphorylated sugar intermediate [1]. While showing similar properties in structure
37 and reaction mechanism, these enzymes differ strongly in substrate specificity. Based on their
38 preferred substrate, the αPHMs are traditionally divided into four main groups: (1)
39 Phosphoglucomutases (PGM), (2) phosphoglucosamine mutases (PNGM), (3)
40 phosphoacetylglucosamine mutases (PAGM) and (4), the group of bifunctional
41 phosphoglucomutases/phosphomannomutases (PGM/PMM) [1]. The most recent expansion to
42 this classification has been the discovery of the mammalian phosphopentomutase (PGM2)
43 and Glucose-1,6-Bisphosphate-synthase (PGM2L1) [2, 3]. This classification, however, lacks a
44 more detailed subdivision in between the main groups and also does not take into account
45 αPHMs preferably catalyzing other reactions (e.g. straight phosphomannomutases) [3]. The
46 NCBI conserved domain database (CDD), instead, classifies the αPHM superfamily in 11
47 different subfamilies on a phylogenetic basis [4]. This phylogenetic model enables a more
48 detailed classification and includes several groups of bacterial and archaeal enzymes showing
49 typical αPHM properties but being only poorly characterized (**Table 1**).
50

CDD group name	CDD identifier	Proposed main function
PGM1	cd03085	Phosphoglucomutase
PGM2	cd05799	Phosphopentomutase (PGM2)/Glc-1,6-BP synthase (PGM2L1)
PGM3(PAGM)	cd03086	Phosphoacetylglucosamine mutase
PMM/PGM	cd03089	Bi-functional phosphomanno-/phosphoglucomutase
PGM like 1	cd03087	Unknown
PGM like 2	cd05800	Unknown
PGM like 3	cd05801	Phosphoglucomutase
PGM like 4	cd05803	Unknown
ManB	cd03088	Phosphomannomutase
GlmM	cd05802	Phosphoglucosamine mutase
Mpg1 transferase	cd05805	GDP-mannose-pyrophosphorylase

Table 1: Subfamilies in the αPHM superfamily with their identifier and proposed main function according to the NCBI conserved domain database (CDD)

51 The PGM (cd03085) from rabbit and human as well as the bacterial PGM (cd05801) from
52 *Salmonella typhimurium* and the bacterial bifunctional PMM/PGM (cd03089) from
53 *Pseudomonas aeruginosa* are among the best characterized αPHMs with available crystal
54 structures and detailed description of reaction mechanisms [5-9]. Catalyzing the interconversion
55 of α-D-glucose-1P (Glc-1P) and α-D-glucose-6P (Glc-6P) makes PGM a key enzyme in glycogen
56 metabolism, glycolysis and gluconeogenesis. During this reaction, a phosphoserine at the
57 active site of PGM donates the phosphoryl group to the substrate Glc-6P or Glc-1P resulting
58 in the synthesis of the transient intermediate α-D-glucose-1,6-bisphosphate (Glc-1,6-BP).
59 After a reorientation in the catalytic center, the intermediate product re-phosphorylates the
60 active site serine yielding Glc-1P or Glc-6P, respectively. Glc-1,6-BP itself acts as an essential
61 activator of PGM by providing an initial phosphorylation of the active site and was first
62 discovered by Leloir, Trucco [10] in yeast extract [11]. While Glc-1,6-BP is not a free metabolite in
63 any metabolic pathway, it is known to be a potent regulator of several enzymes in central
64 carbon metabolism in eukaryotes: in addition to PGMs and other αPHMs, it was shown to
65 regulate hexokinases, 6-phosphogluconate dehydrogenase, phosphofructokinase and
66 pyruvate kinase [12]. In mammalian tissues the synthesis of Glc-1,6-BP is catalyzed by the
67 PGM2L1 enzyme, a member of the cd05799 subfamily, utilizing 1,3-bisphosphoglyceric acid
68 (1,3-BPG) as phosphoryl donor for Glc-1P [3]. In contrast, despite its essential role in the activity
69 of prokaryotic PGM, the function of Glc-1,6-BP in prokaryotes has been overlooked and its
70 origin remains obscure as no enzyme producing free Glc-1,6-BP has been identified so far [13].
71 The unicellular cyanobacterium *Synechocystis* sp. PCC 6803 (hereafter *Synechocystis*) has two
72 enzymes that are encoded by the genes *sll0726* and *slr1334* and annotated as PGM-like [4].
73 While Sll0726 exhibits typical properties of PGMs [14-16], little is known about Slr1334. The only
74 study addressing this issue reported that purified *Synechocystis* Sll0726 has about a tenfold
75 higher activity *in vitro* than Slr1334 and that a *sll0726* knockout mutant only shows around
76 3 % PGM activity compared to the wildtype [17]. Despite its low contribution to over-all PGM
77 activity, the Slr1334 product appeared to be essential as it was not possible to acquire fully
78 segregated knockout mutants of the *slr1334* gene, which raised the question of the role of
79 Slr1334 in *Synechocystis*.
80
81 In this work we show that Slr1334 has a phosphotransferase activity catalyzing the production
82 of free Glc-1,6-BP from Glc-1P/Glc-6P and Fructose-1,6-bisphosphate (Frc-1,6-BP). Thereby,

Slr1334 is responsible for the formation of the key activator of PGM, Glc-1,6-BP, making it a major regulator in glycolysis and other carbon pathways. Our finding makes Slr1334 the first bacterial enzyme specific for the production of free Glc-1,6-BP. Importantly, we show that the homologue of Slr1334 in the human gut bacterium *Bacteroides salyersiae* catalyzes the same reaction.

Results

Classification of the two PGM isoenzymes from *Synechocystis*

Synechocystis possesses two genes annotated as PGMs, the genes *sll0726* and *slr1334*. In order to classify them within the αPHM superfamily, we performed a phylogenetic analysis by multi-level alignment of all αPHM subfamilies that are considered PGM or "PGM_like". For this, we collected the entry sequences from the NCBI Conserved Domains Database (CDD) [4] and retrieved further sequences by performing BLAST searches in the NCBI RefSeq_protein database. To focus on glucose-specific αPHMs, the groups of enzymes specific for other sugars like PMMs, PNGM and PAGMs (cd03086 cd03088, cd05802, cd05805) were omitted from the analysis (**Fig. 1**). In general the αPHMs can be divided into four conserved regions which are from N- to C-terminus: (1) the active site domain, (2) the metal binding domain, (3) the sugar binding domain and (4) the phosphate binding domain. While the domains 1,2 and 4 are usually highly conserved between the different subfamilies, the sugar binding domain shows a greater variance and can assist in the categorization of αPHMs (**Table S1**) [2].

Slr1334 is part of the cd05800 (PGM like 2) subfamily present in many bacterial groups. In agreement with the CDD, our phylogenetic analysis shows that this subfamily forms a distinct cluster of PGMs which clearly separates from other PGM and PGM like enzymes. The Sll0726 PGM, by contrast, is a member of the cd05801 subfamily, to which the well characterized PGM from *S. typhimurium* belongs.

113

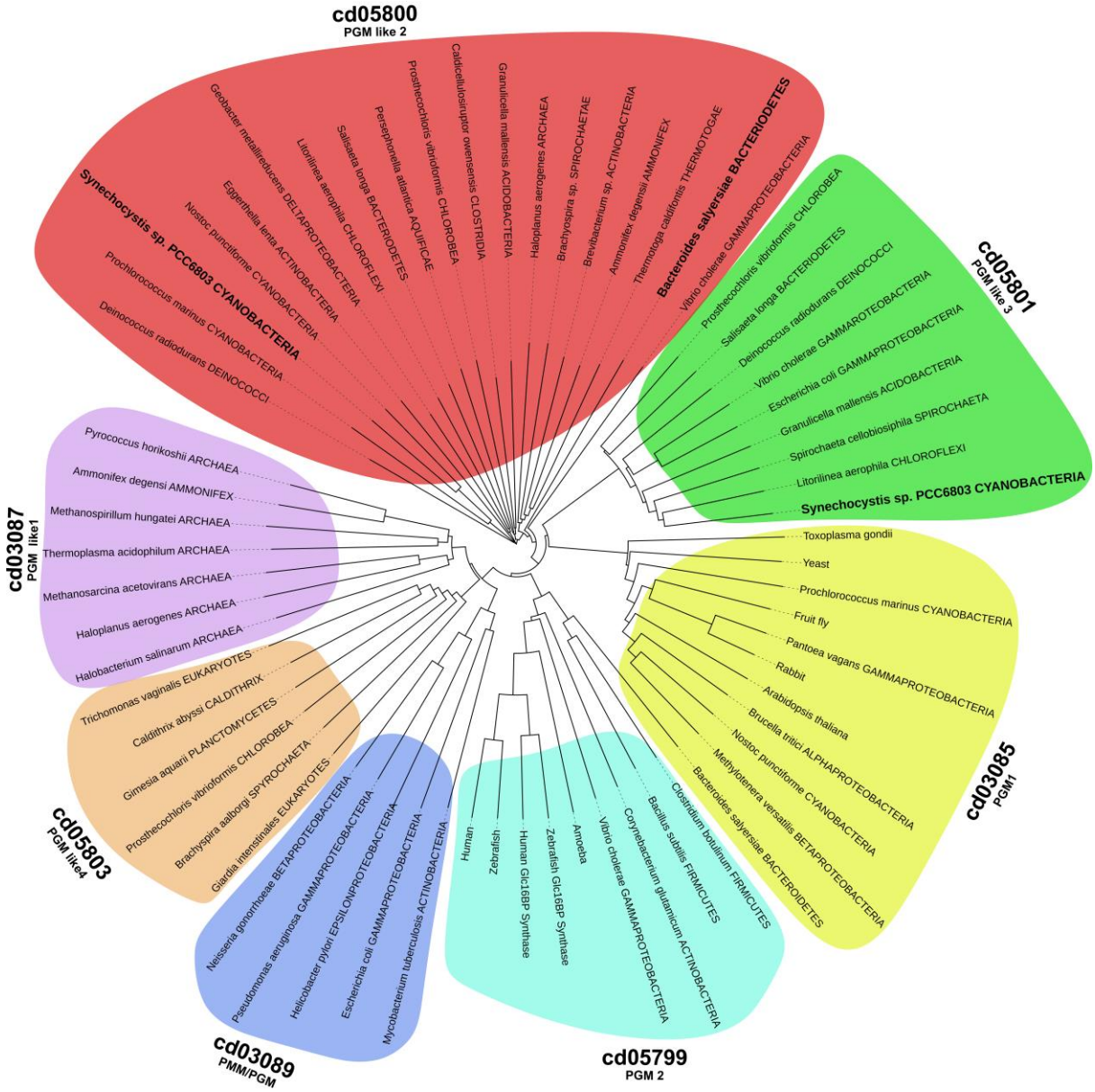

Figure 1: **Phylogenetic tree of the αPHM subfamilies that are considered to be "PGM-like" according to CDD**

The tree was built on the taxonomy based on the protein sequences present in the NCBI RefSeq_protein database. The CDD subfamilies cd03086, cd03088, cd05802 and cd05805, which are known to catalyze distinct reactions, were omitted from the analysis. The organisms investigated in this study are highlighted in bold letters.

114

115 **Slr1334 shows low PGM activity compared to Sll0726 but behaves differently in presence**
116 **of Fructose-1,6-BP**

117 To gain deeper insights into the role of the enigmatic Slr1334, we overexpressed Sll0726 along
118 with Slr1334 in *Escherichia coli* and assessed the PGM enzymatic activity of the purified
119 proteins by measuring the interconversion of Glc-1-P to Glc-6-P in an assay that couples Glc-
120 6-P formation to its subsequent oxidation using Glucose-6-phosphate-dehydrogenase
121 (G6PDH) and $NADP^+$. We could show that Slr1334 only displays about 5% of catalytic efficiency
122 compared to Sll0726 when both PGMs were tested with saturating amounts of the activator
123 Glc-1,6-BP (60 µM) (**Fig. 2, Table 2. See also Fig. 3**). Interestingly, the PGM activity of both
124 enzymes was also measurable without addition of Glc-1,6-BP, which is considered to be an
125 essential activator. However, in the absence of Glc-1,6-BP, the catalytic efficiency was about
126 70 times lower due to a significantly increased Michaelis-Menten constant (K_m) for Sll0726 and
127 Slr1334 alike.
128 Fructose-1,6- bisphosphate is an endogenous intermediate of the glycolytic pathway and is
129 known to be an inhibitor of PGM most likely by competing with the reaction intermediate Glc-
130 1,6-BP [18, 19]. In a preliminary experiment we tested the effect of different concentrations of
131 Frc-1,6-BP on Sll0726 and observed major inhibition already at concentrations of 100 µM (data
132 not shown). When testing PGM activity by replacing 60 µM Glc-1,6-BP with 100 µM Frc-1,6-
133 BP, we detected a decrease in catalytic efficiency to 19 % as a consequence of a strongly
134 increased K_m (**Fig. 2, Table 2**). Strikingly, however, for Slr1334 we detected a different effect:
135 while the catalytic rate constant (k_{cat}) decreased by about 2-fold, we measured an
136 approximately 100-fold reduced K_m resulting in a 50 times increased catalytic efficiency. This
137 raised the question of how Frc-1,6-BP affected the PGM-activity of Slr1334. We speculated
138 that Frc-1,6-BP might either function as a direct activator similar to Glc-1,6-BP or be required
139 for the synthesis of the activating compound Glc-1,6-BP during the reaction of Slr1334. As we
140 will show below, the activating compound turned out to be Glc-1,6-BP and not Frc-1,6-BP.
141
142
143
144
145
146

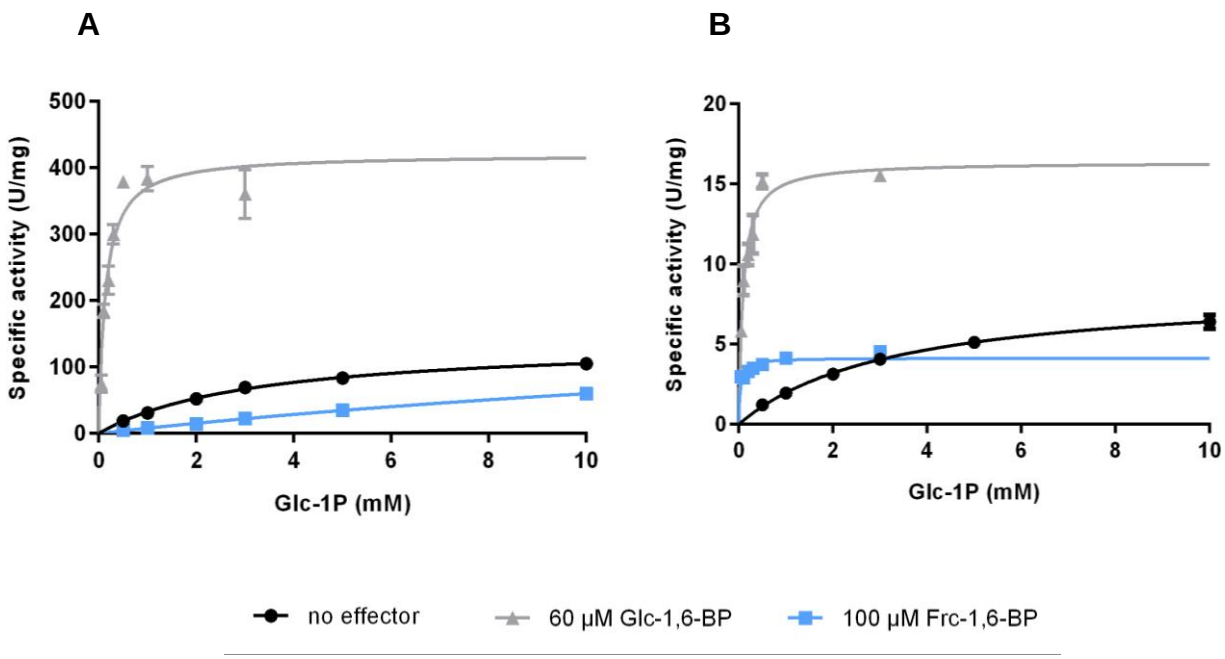

Figure 2: Slr1334 shows lower PGM activity then Sll0726 and behaves differently in presence of Frc-1,6-BP

Shown are the Michaelis-Menten kinetics of Sll0726 (A) and Slr1334 (B): in black, without addition of effectors; in light grey in the presence of 60 µM Glc-1,6-BP; in blue, in the presence of 100 µM Frc-1,6-BP. Three replicates were measured for each data-point. Error bars represent the SD.

Effector	Sll0726			Slr1334			
	K_m (mM)	k_{cat} (s^{-1})	k_{cat}/K_m ($M^{-1}s^{-1}$)	K_m (mM)	k_{cat} (s^{-1})	k_{cat}/K_m ($M^{-1}s^{-1}$)	Catalytic efficiency ratio (%) (Slr1334/Sll0726)
No effector	3.27 ± 0.21	138 ± 3.7	42.2 *10^3	3.31 ± 0.14	7.5 ± 0.1	2.3 * 10^3	**5.5**
Glc-1,6-BP	0.19 ± 0.04	415 ± 30.6	3038.9 * 10^3	0.09 ± 0.02	14.4 ± 0.7	158.1 * 10^3	**5.2**
Frc-1,6-BP	26.86 ± 3.35	218 ± 21.3	8.1 * 10^3	0.03 ± 0.01	3.6 ± 0.2	117.5 * 10^3	**1450**

Table 2: Kinetic parameters of Sll0726 and Slr1334 with different effector molecules
K_m and K_{cat} values are means of triplicates with ± SD. Catalytic efficiency ratio is given in percentage and was calculated by the ratio of K_{cat}/K_m of Slr1334 and Sll0726.

172 **Slr1334 forms a product out of Frc-1,6-BP and Glc-1P/Glc-6P that strongly activates Sll0726**

173 To determine the amount of Glc-1,6-BP needed to achieve activation of Sll0726 at 1 mM Glc-
174 1P we first tested enzymatic activity of Sll0726 at different Glc-1,6-BP concentrations.
175 Maximum activation was achieved at Glc-1,6-BP concentrations between 30 and 60 µM
176 resulting in a 5-fold increased activity as compared to the zero Glc-1,6-BP reaction (**Fig. 3**).
177 Next, we incubated Slr1334 with the phosphorylated sugars Frc-1,6-BP, Glc-1P and Glc-6P (1
178 mM each) in different combinations and subsequently tested whether Sll0726 could be
179 activated by the corresponding reaction products (**Fig. 3**). As negative control, Frc-1,6-BP and
180 Glc-1P were allowed to react without any enzyme or with Sll0726 instead of Slr1334. After
181 running the Slr1334 reaction for 1.5 h, the reaction was stopped by heat inactivation and the
182 supernatant was added in a dilution of 1:10 to the reaction mixture of the Sll0726 assay, which
183 was then started by adding 1 mM Glc-1P. Only after adding the supernatant of the Slr1334
184 reaction containing Frc-1,6-BP and Glc-1P (or Glc-6P) as substrates, the velocity of the Sll0726
185 reaction was increased by 5-fold in comparison to the control reaction at zero Glc-1,6-BP (**Fig.**
186 **3**). When the Sll0726 test reaction was performed with the supernatant of the Sll0726 control
187 reaction or the reaction products of Slr1334 using Frc-1,6-BP as sole substrate, the enzyme
188 velocity was lower than the zero Glc-1,6-BP reaction. This reduction can be explained by the
189 inhibitory effect of Frc-1,6-BP on Sll0726, as exemplified by the "no enzyme control" reaction
190 (**Fig. 3**).
191
192 In addition to Frc-1,6-BP, we also tested whether Slr1334 can utilize 1,3-BPG instead of Frc-
193 1,6-BP for Glc-1,6-BP formation as described for the mammalian PGM2L1. Since 1,3-BPG is not
194 commercially available, we established an assay whereby we continuously produced 1,3-BPG
195 by a phosphoglycerate kinase (PGK) reaction using a His-tagged purified PGK in combination
196 with 1 mM 3PG and 1 mM ATP (see methods part). This reaction was directly coupled to the
197 reaction of Slr1334 with Glc-1P or Glc-6P or no substrate. As a control the same reaction was
198 performed with Sll0726 instead of Slr1334. To test the possible formation of Glc-1,6-BP, the
199 supernatants of these reactions were added to the Sll0726 reaction before performing the
200 enzymatic assay as described above.
201 We detected an increase in Sll0726 activity by approx. 2.5-fold compared to the zero Glc-1,6-
202 BP reaction when the supernatant of the Slr1334 reaction contained 1,3-BPG and either Glc-
203 1P or Glc-6P. No increase in activity was detected when the supernatant solely contained 1,3-

204 BPG. The supernatant of the control reaction with Sll0726 instead of Slr1334 resulted in no
205 marked change in activity.
206 By comparing the activation of Sll0726 by the Slr1334 reaction products to the activation of
207 Sll0726 at different concentration of Glc-1,6-BP we could estimate the efficiency of Glc-1,6-BP
208 formation from Frc-1,6-BP or 1,3-BPG. With Frc-1,6-BP as substrate for the Slr1334 reaction,
209 a maximum activation of Sll0726 was achieved, which corresponded to activation of Sll0726
210 with concentrations of Glc-1,6-BP between 30 and 60 µM (**Fig. 3**). When 1,3-BPG was used as
211 substrate as described above, the increase in Sll0726 activity corresponded to Glc-1,6-BP
212 concentrations between 1 and 5 µM. From this experiment we conclude that i) Slr1334 forms
213 a product out of Glc-1P/Glc-6P and either Frc-1,6-BP or 1,3-BPG that is able to activate Sll0726
214 similar to defined amounts of Glc-1,6-BP; ii) when normalizing the Sll0726 activation to Glc-
215 1,6-BP concentrations, the reaction product of Slr1334 using Frc-1,6-BP as phosphorylating
216 sugar is 10-fold more effective in activating Sll0726 than using 1,3-BPG.
217
218
219
220
221
222
223
224
225
226

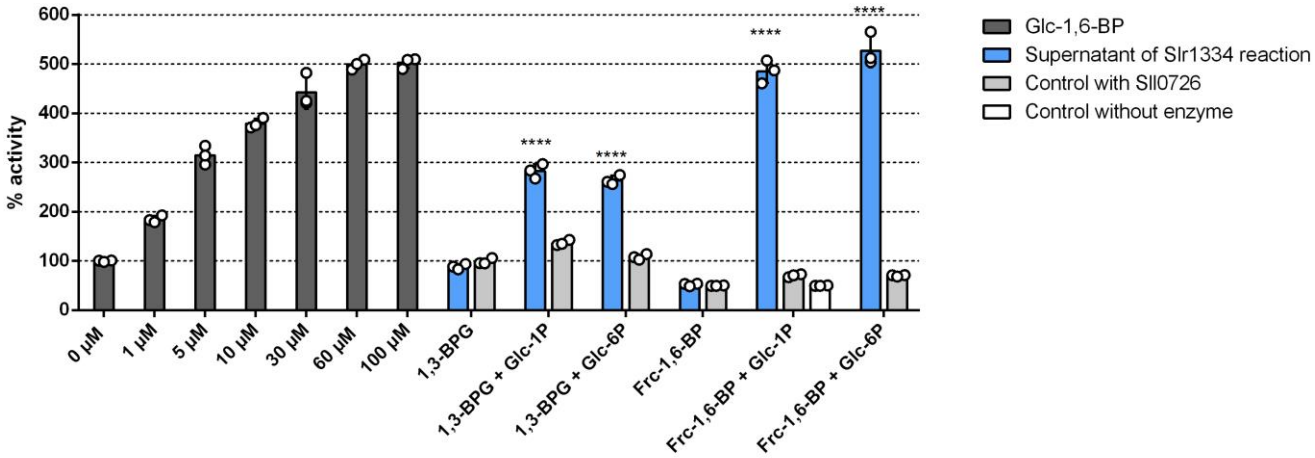

227
228 **Figure 3: Slr1334 produces a compound out of Frc-1,6-BP that strongly activates Sll0726**

229 Shown is the Sll0726 activity: in dark grey, at different Glc-1,6-BP concentrations; in blue,
230 after addition of the supernatant of the Slr1334 reaction; in light grey, after addition of the
231 supernatant of the Sll0726 reaction as a control; in white, after addition of the sole
232 phosphosugars without enzyme as further control. The different combinations of
233 substrates used for the Slr1334 reaction and controls are indicated on the X-axis. Values
represent relative activity compared to the Sll0726 reaction with 0 µM Glc-1,6-BP, which
was considered 100%. Three biological replicates were measured for each datapoint. Error
bars represent the SD; asterisks represent the statistical significance.

234

235 **The product of the Slr1334 reaction is not degradable by the Frc-1,6-BP-aldolase**

236 To confirm that the activating compound formed from Glc-1P/Glc-6P and Frc-1,6-BP through
237 the Slr1334 reaction is in fact Glc-1,6-BP, we analyzed the reaction product via liquid
238 chromatography-mass spectrometry (LC/MS). Therefore, we incubated Slr1334 together with
239 500 µM Frc-1,6-BP and 1 mM Glc-1P for 1.5 h. As a control, the same substrates were
240 incubated without enzyme. Since LC/MS analysis does not allow discriminating Glc-1,6-BP
241 from Frc-1,6-BP, we performed an additional reaction step to specifically degrade Frc-1,6-BP.
242 Therefore, after heat inactivation, the reaction mixture was incubated with Frc-1,6-BP-
243 aldolase (Fba) and glycerol-3-phosphate-dehydrogenase (GPDH) as well as 1 mM NADH: Fba
244 specifically cleaves Frc-1,6-BP into dihydroxyacetone phosphate (DHAP) and glyceraldehyde-
245 3P while Glc-1,6-BP is unaffected. GPDH subsequently forms glycerol-3-phosphate (glycerol-
246 3P) and NAD^+ out of DHAP and NADH. This is necessary to enable full degradation of Frc-1,6-
247 BP.
248 After this treatment, LC/MS analysis revealed that a compound with a mass corresponding to
249 either Glc-1,6-BP or Frc-1,6-BP was present in the Slr1334 reaction while this mass was not
250 detectable in the control reaction where no Slr1334 was present (**Fig. 4**). This indicates that
251 Frc-1,6-BP in the control reaction was completely degraded in the subsequent reaction by Fba
252 as expected, while Frc-1,6-BP in the Slr1334 reaction was metabolized into a molecule of the
253 same mass that was not degraded by Fba. This is precisely what is expected when Glc-1,6-BP
254 is produced form Frc-1,6-BP turn-over. Furthermore, the reaction products from the coupled
255 GPDH reaction, NAD+ and glycerol-3P were more abundant in the control reaction without
256 Slr1334 as compared to the reaction with Slr1334. This indicated that more Frc-1,6-BP was
257 degraded out of the control reaction than out of the reaction containing Slr1334 due to partial
258 conversion of Frc-1,6-BP into Glc-1,6-BP by Slr1334 (**Fig. 4**). Altogether, this experiment
259 strongly indicated that in the presence of Slr1334, Frc-1,6-BP was partially utilized to form Glc-
260 1,6-BP. The fact that only a part of Frc-1,6-BP was consumed could be either due to a too short
261 reaction time or because the reaction reached an equilibrium state.
262
263
264
265
266

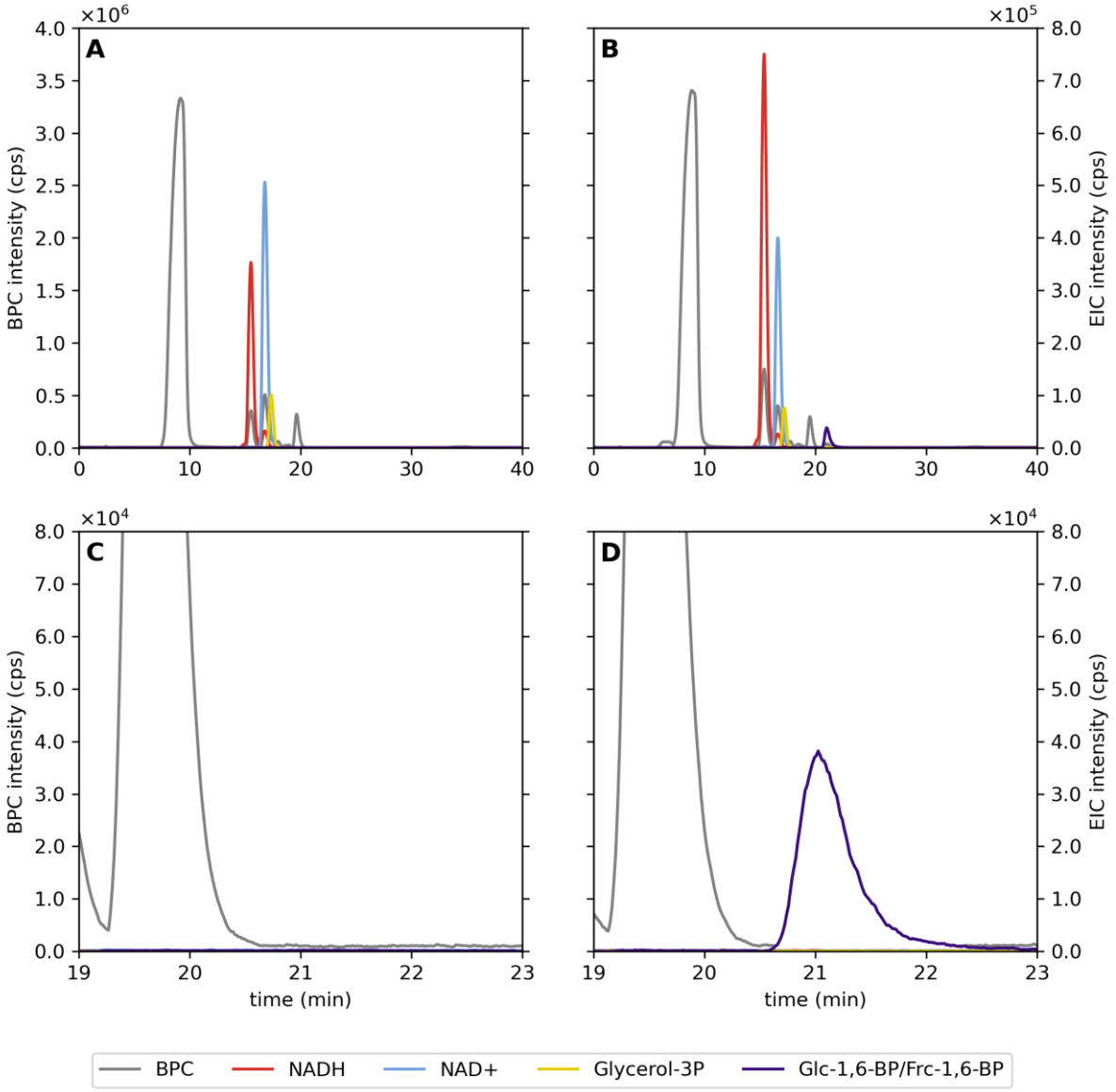

Figure 4: LC-MS analysis reveals that Slr1334 metabolizes Frc-1,6-BP into a molecule of identical mass that is not degraded by Frc-1,6-BP-aldolase

Analysis of the products of the reaction without (A) and with Slr1334 (B) via LC/MS. Shown are the base peak chromatograms (BPC) in the mass range $(M\text{-}H)^-$ m/z = 79–1,601 (grey) and the extracted ion chromatograms (EIC) based on the exact masses of NAD+ $(M\text{-}H)^-$= 662.101 m/z (light blue), NADH $(M\text{-}H)^-$= 664.117 m/z (red), Glycerol 3-P $(M\text{-}H)^-$= 171.006 m/z (yellow), Glc-1,6-BP/Frc-1,6-BP $(M\text{-}H)^-$= 338.988 m/z (purple). The presence of the NAD+ (blue) and Glycerol-3P (yellow) peaks in (B) shows that Frc-1,6-BP was not fully metabolized into Glc-1,6-BP. Magnification and adjustment of the graphs in (A) and (B) is clear evidence of the absence (C) or formation (D) of Glc-1,6-BP.

298 For investigating whether the formation of Glc-1,6-BP out of Glc-1P/Glc-6P and Frc-1,6-BP is
299 an equilibrium reaction, we performed an enzymatic assay to determine the amount of the
300 remaining Frc-1,6-BP. Therefore, Slr1334 was incubated with 500 µM of Frc-1,6-BP and 1 mM
301 Glc-1P for 1.5 h. As controls, the same assays were performed with Sll0726 or without any
302 enzyme. After the reaction was stopped by heat inactivation, the supernatant was used to run
303 the coupled Fba/GPDH assay in a dilution of 1:10, which would correspond to a final
304 concentration of 50 µM Frc-1,6-BP if no Frc-1,6-BP was consumed. As further controls,
305 standards of 50 µM and 25 µM Frc-1,6-BP were used in the Fba/GPDH assay. This experiment
306 showed that the concentration of Frc-1,6-BP decreased by about 50 % when in the first
307 reaction Slr1334 was present, while apparently no Frc-1,6-BP was utilized in the control
308 reactions (**Fig. 5**). This result agreed with the assumption that the reaction reaches an
309 equilibrium at 50 % product formation, either because of the reversibility of the reaction or
310 product inhibition.
311
312
313
314
315
316
317
318
319
320
321
322

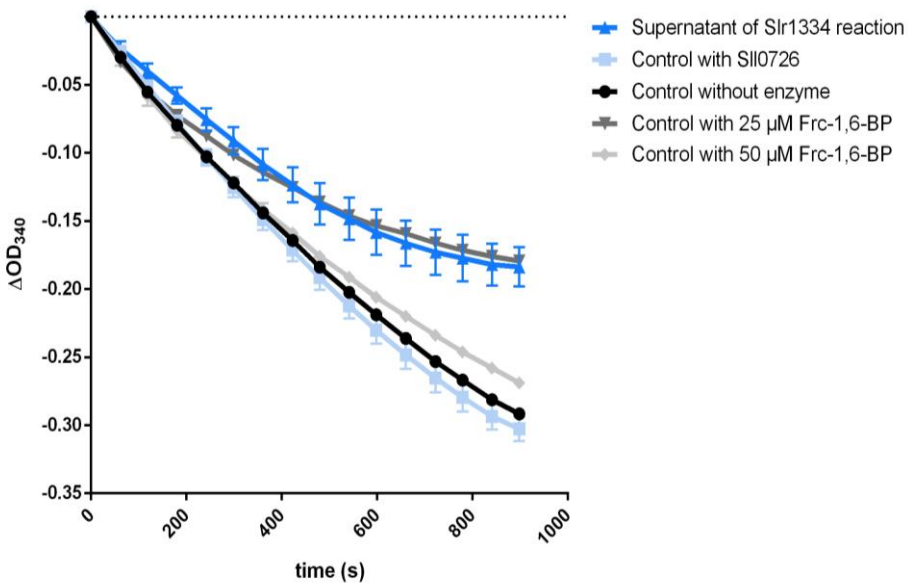

323 **Figure 5: Slr1334 produces Glc-1,6-BP out of Frc-1,6-BP in an equilibrium reaction**

324 Shown is the Frc-1,6-BP-aldolase activity: in dark blue, after addition of the supernatant of
325 the Slr1334 reaction; in light blue, after addition of the supernatant of the Sll0726 reaction
326 as a control; in black, after addition of the supernatant without any enzyme. In dark grey
327 and light grey, the aldolase activity measured at Frc-1,6-BP concentrations of 25 µM and
50 µM, respectively, as further control.
328 Frc-1,6-BP was used at concentrations of 500 µM in the Slr1334 reaction and respective
329 control reactions. Therefore, its final concentration in the Sll0726 assay after 1:10 dilution
was expected to be 50 µM assuming no consumption of Frc-1,6-BP in the Slr1334 reaction.
Three replicates were measured for each datapoint. Error bars represent the SD.

330 **The Slr1334 reaction is reversible**

331 To reveal whether Slr1334 can catalyze the proposed reverse reaction and synthesize Frc-1,6-
332 BP from Glc-1,6-BP and Fructose-1P (Frc-1P)/Fructose-6P (Frc-6P), formation of Frc-1,6-BP was
333 coupled to the Fba and GPDH reaction. For the assay, 50 µM Glc-1,6-BP was used and the
334 reaction was started by the addition of 5 mM Frc-6-P. As control reactions, *Synechocystis*
335 Sll0726 as well as PGM1 from rabbit were used. The results clearly showed that Slr1334 could
336 produce Frc-1,6-BP, resulting in measurable aldolase activity while the controls showed no
337 activity (**Fig. 6a**). Using this assay, we tried to determine the kinetic constants for the two
338 substrates Frc-6-P and Glc-1,6-BP. For Frc-6P, a K_m of 1 mM and a K_{cat} of 1.2 s^{-1} could be
339 determined (**Fig. 6b, Table 3**). By contrast, the affinity of Slr1334 for Glc-1,6-BP was so high
340 that, even at the lowest measurable substrate concentrations (2 µM), the reaction proceeded
341 with maximal velocity (**Fig. 6c**). Altogether these experiments unequivocally demonstrate that
342 Slr1334 is the first characterized bacterial Glc-1,6-BP synthase. In contrast to the eukaryotic
343 Glc-1,6-BP synthase, the prokaryotic enzyme uses Frc-1,6-BP as major phosphoryl donor for
344 Glc-1,6-BP production.
345
346
347
348
349
350
351
352
353
354
355
356
357
358
359
360
361

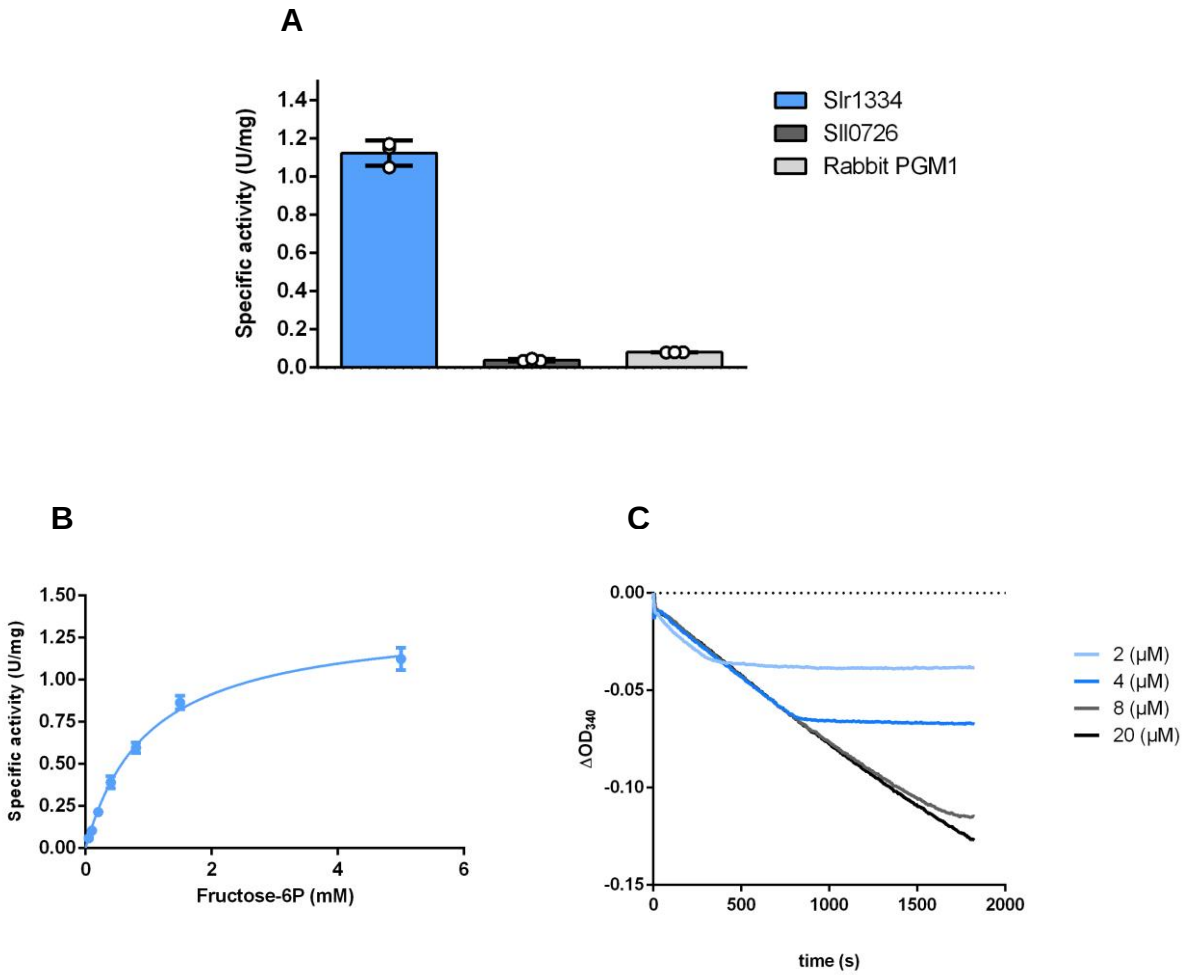

Figure 6: Slr1334 catalyzes the reverse reaction to form Frc-1,6-BP out of Glc-1,6-BP and Frc-6P

(A) Activity of Slr1334 (blue), Sll0726 (grey), and rabbit PGM1 (black) using 50 µM Glc-1,6-BP and 5 mM Frc-6P. (B) Michaelis-Menten kinetics of Slr1334 using different concentrations of Frc-6P and 50 µM Glc-1,6-BP. (C) Slr1334 reaction at different concentrations of Glc-1,6-BP and 0.5 mM Frc-6P. Three replicates were measured for each datapoint. Error bars represent the SD; asterisks represent the statistical significance.

Substrate	**K_m (mM)**	**k_{cat} (s^{-1})**	**k_{cat}/K_m ($M^{-1}s^{-1}$)**
Glc-1,6-BP	<0.002	1.2 ± 0.03	600000
Frc-6P	1.0 ± 0.07		>1200

Table 3: Kinetic parameters of Frc-1,6-BP synthesis by Slr1334
K_m and Kcat values are means of triplicates with ± SD.

392 **The Glc-1,6-BP synthase reaction is also performed by other members of the cd05800 group**

393 To determine whether the reaction catalyzed by Slr1334 is representative for αPHM enzymes
394 of the cd05800 family, we decided to analyze the corresponding homologue from the human
395 microbiome associated bacterium *Bacteroides salyersiae*. Therefore, we tested formation of
396 Glc-1,6-BP under the same conditions as described above for Slr1334 by incubating the
397 recombinant cd05800 enzyme from *B. salyersiae* with Frc-1,6-BP and Glc-1P or Glc-6P and
398 subsequently adding the supernatant of this reaction to the Sll0726 assay. As a positive control
399 we used the reaction of Slr1334.
400 The addition of the supernatant from the *B. salyersiae* cd05800 PGM increased the velocity of
401 Sll0726 in a comparable manner as the supernatant of the Slr1334 reaction (**Fig. 7**). This
402 indicates that similar amounts of Glc-1,6-BP have been formed in both reactions, hence
403 revealing that *B. salyersiae* cd05800 PGM catalyzes the same reaction as Slr1334.
404
405
406
407
408
409
410
411
412
413
414
415
416
417

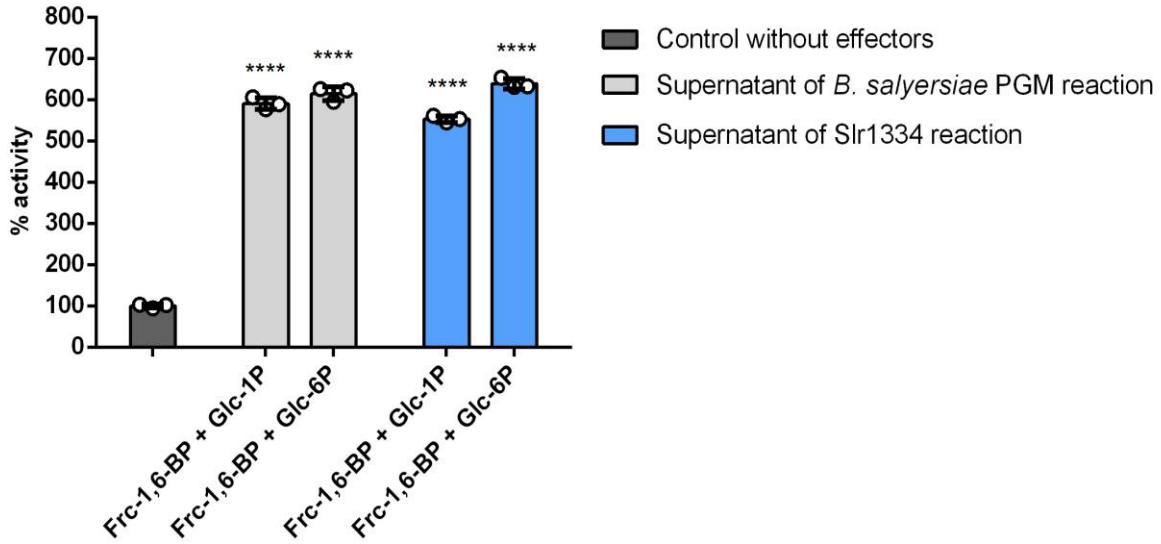

418 **Figure 7: Slr1334 homologue from *B. salyersiae* also forms Glc-1,6-BP out of Frc-1,6-BP**

419 Shown is the activity of Sll0726: blue, after addition of the supernatant of the *B. salyersiae*
420 PGM reaction; in light grey, after addition of the supernatant of the Slr1334 reaction as a
positive control; in dark grey, without any effectors as a negative control. The different
421 combinations of substrates used for the *B. salyersiae* PGM and Slr1334 control reaction are
indicated on the X-axis. Values represent relative activity compared to the Sll0726 reaction
without any effectors, which was considered 100%. Error bars represent the SD; asterisks
422 represent the statistical significance.

423 ## Discussion

424 Among the key reactions in carbon metabolism are the phosphoryl transfer reactions on
425 different phosphosugars, which are catalyzed by the members of the αPHM superfamily.
426 These reactions are essential for glycogen metabolism, amino sugar metabolism as well as cell
427 wall synthesis and are conserved throughout all domains of life. The interconversion of Glc-1P
428 to Glc-6P and vice versa by PGM is by far the best studied of these reactions and investigation
429 of PGM goes back to the 1940s. It has long been known that PGM requires Glc-1,6-BP as a
430 activator [10]. While in mammals free Glc-1,6-BP has been shown to derive from the reaction of
431 the PGM2L1 enzyme utilizing Glc-1P and 1,3-BPG as substrates, its origin in prokaryotes has
432 remained unknown [3].
433 In this study we used the unicellular cyanobacterium *Synechocystis* sp. PCC6803 as a model
434 organism to identify the first bacterial glucose-1,6-BP synthase. This reversible reaction is a
435 novel function of a member of a distinct αPHM subfamily producing free α-D-Glc-1,6-BP and
436 Frc-6P from Frc-1,6-BP and Glc-1P/Glc-6P.
437 Glc-1,6-BP is essential for PGM activity due to the requirement for phosphorylation of the
438 serine residue at the active site for enzyme activation. The activating reaction converts Glc-
439 1,6-BP into either Glc-1P or Glc-6P. After this initial activation, the interconversion of Glc-1P
440 to Glc-6P is mediated by a transfer of the phosphate group from the serine residue at the
441 active site to the 1' or 6' position of the substrate respectively, forming a Glc-1,6-BP
442 intermediate. This intermediate has to reconfigure inside the enzyme and transfer the
443 phosphate of its 6' or 1' position back to the active site serine leading to the release of Glc-6P
444 or Glc-1P, respectively. As a result of this mechanism, the active site remains phosphorylated
445 and the enzyme is ready for a new cycle. However, it has been shown that the phosphorylation
446 of PGM at the active site is lost after an average of 15-20 reaction cycles by a spontaneous
447 dissociation of the intermediate Glc-1,6-BP leaving behind an inactive dephosphoenzyme.
448 Therefore, a constant level of Glc-1,6-BP is necessary to ensure that PGM is kept in an active
449 state [20, 21]. While the loss of the intermediate might be regarded as an unfavorable event, it
450 can also be considered as a regulatory mechanism that enables regulation of PGM activity
451 based on Glc-1,6-BP levels. For other αPHMs like PMM and PNGM it is known that the
452 corresponding intermediates (e.g. α-D-mannose-1,6-BP and α-D-glucosamine-1,6-BP) are
453 formed during the reaction of the respective enzymes in the same way as for PGM but no

454 source of those intermediates is known that would enable an initial activation of these αPHMs
455 or would keep them in an active state overtime when phosphorylation is lost. However, since
456 many members of the αPHM family show at least some residual PGM activity, Glc-1,6-BP was
457 suggested to be the activating compound for these enzymes as well. This has in fact been
458 shown for PNGM from *E. coli* which is considered to be an essential enzyme [22]. This makes the
459 role of Glc-1,6-BP in carbon metabolism even more relevant and would explain the failed
460 attempts to delete the *slr1334* gene [17].
461 In mammals, it was shown that Glc-1,6-BP can also regulate central enzymes of carbon
462 pathways by inhibiting hexokinases, 6-phosphogluconate dehydrogenase and fructose-1,6-
463 bisphosphatase and by activating phosphofructokinase and pyruvate kinase [12]. Further studies
464 in mammals showed that Glc-1,6-BP is especially elevated in brain tissue to a level that highly
465 exceeds the regulatory concentrations needed for PGM activity, and that reduced levels of
466 Glc-1,6-BP cause severe neurological problems [23]. This indicates that at least in mammals
467 there are likely more functions of Glc-1,6-BP to be discovered. Given the important role of Glc-
468 1,6-BP in eukaryotic metabolism, it is surprising that very little is known on the role of Glc-1,6-
469 BP in bacterial physiology. The only study about the origin of α-D-Glc-1,6-BP production in
470 bacteria proposed a phosphodismutase reaction with Glc-1P as the sole substrate in *E. coli* [24].
471 Moreover, the levels of Glc-1,6-BP in eukaryotes are affected by a specific Glc-1,6-BP
472 phosphatase, PMM1, which is a phosphomannomutase that is not part of the αPHM
473 superfamily. Whether a homologue exists in bacteria is currently unknown [25].
474 In absence of Glc-1,6-BP, both Slr1334 and Sll0726 showed low PGM activity. This residual
475 activity can be explained by the fact that a phosphorylation of the active site serine can also
476 be achieved at high concentrations of Glc-1P but at a much lower efficiency, leading to high
477 K_m values and overall strongly reduced activity [11]. In the presence of Frc-1,6-BP, Sll0726 was
478 strongly inhibited, which agrees with the inhibitory effect of Frc-1,6-BP on other PGMs [19, 26].
479 By contrast, Frc-1,6-BP enhanced the overall catalytic activity of Slr1334, primarily because of
480 a strongly decreased K_m. This effect can now be attributed to the formation of the activator
481 Glc-1,6-BP.
482 Like mammalian PGM2L1, Slr1334 can utilize 1,3-BPG as a phosphorylating compound for Glc-
483 1,6-BP formation, however with a much lower efficiency than with Frc-1,6-BP. For the
484 mammalian PGM2L1 a reverse reaction (formation of 1,3-BPG and Glc-1P from Glc-1,6-BP and
485 3-PG) has not been shown. For Slr1334, we could clearly show reversibility of the reaction,

486 producing Frc-1,6-BP from Glc-1,6-BP and Frc-6P. Provided that both directions of the reaction
487 have similar kinetic properties, Slr1334 appears to be a *bona-fide* Glc-1,6-BP synthase, which
488 is prone to activate the main PGM Sll0726.
489 In contrast to Glc-1,6-BP, Frc-1,6-BP is an obligatory intermediate in glycolysis,
490 gluconeogenesis and Calvin-Benson-Bassham cycle. In contrast to mammalian PGM2L1,
491 *Synechocystis* Slr1334 uses this sugar as the major substrate for Glc-1,6-BP synthesis. This links
492 the synthesis of Glc-1,6-BP to the levels of Frc-1,6-BP. Its steady state level depends on the
493 activity of the opposing reactions of phosphofructokinase (Pfk) and Fructose-1,6-
494 bisphosphatase (FBPase), both of which are regulated in an opposite manner: While PFK is
495 usually activated by the low energy state metabolites ADP and AMP and downregulated by
496 the high energy state metabolites ATP and citrate, FBPase is downregulated by AMP while
497 unaffected by high energy compounds. The level of Frc-1,6-BP is further determined by the
498 Frc-1,6-BP-aldolase activity. Frc-1,6-BP is also known to be an allosteric activator of pyruvate
499 kinase (PK), the final step in glycolysis [27].
500 Altogether, in the cyanobacterium *Synechocystis* PCC6803, Frc-1,6-BP appears to have two
501 counteracting effects on PGM activity. On the one hand, it acts as a direct inhibitor of PGM;
502 on the other hand, it gives rise to the synthesis of the PGM activator Glc-1,6-BP through the
503 activity of Slr1334. Furthermore, since these double phosphorylated sugars may affect further
504 enzyme reactions, by connecting these two metabolites, Slr1334 might represent a crucial
505 regulatory point in glycolysis (**Fig. 8**). This conclusion would further underline the essential
506 role of *slr1334* [17].
507
508
509
510
511
512
513
514
515
516
517

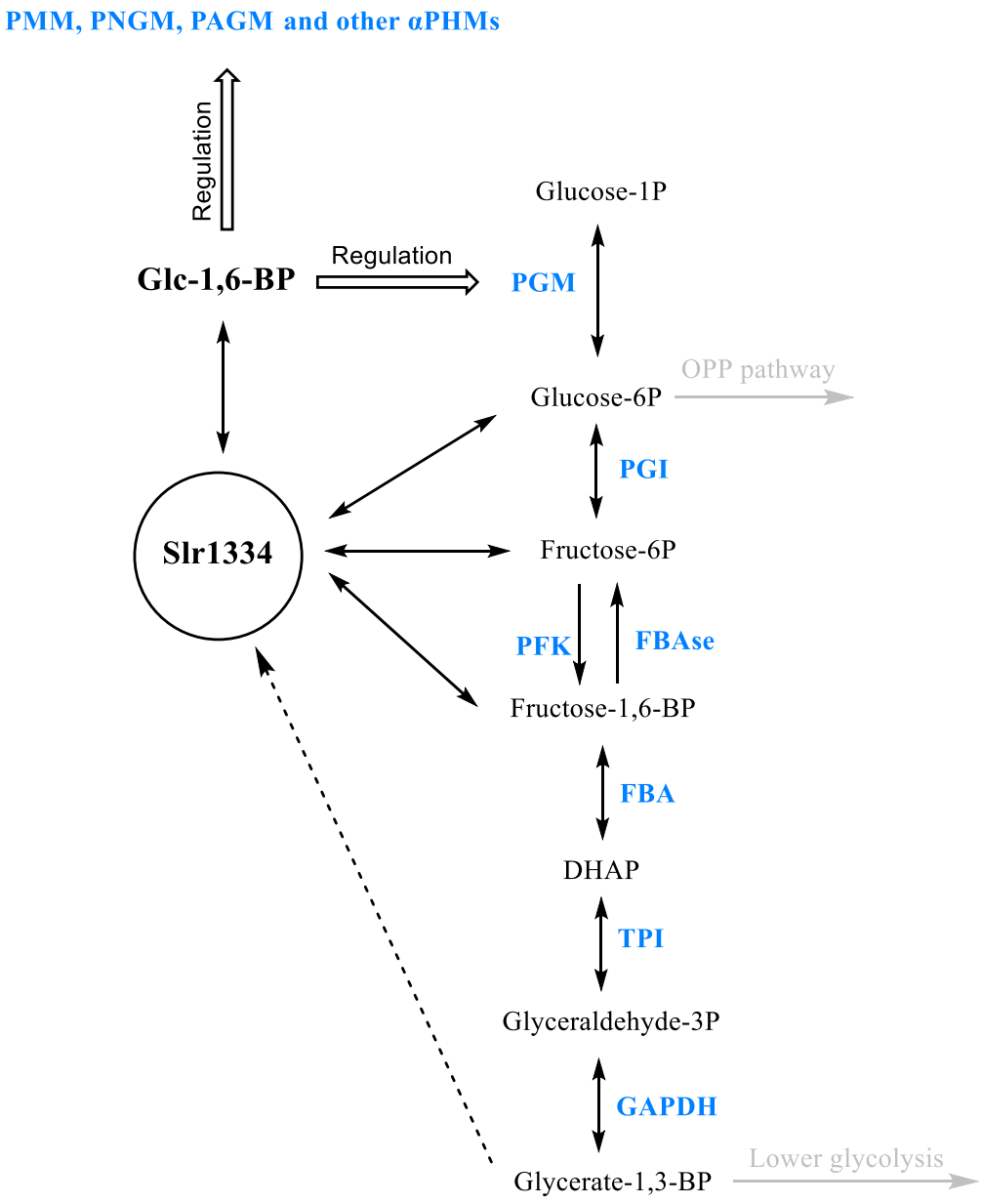

Figure 8: Potential role of Slr1334 in glycolysis

Shown is the potential role of Slr1334 in regulating activity of αPHMs and the concentration of key metabolites in glycolysis. PGM: Phosphoglucomutase; PGI: Glc-6P-Isomerase; PFK: Phosphofruktokinase; FBAse: Fructose-6P phosphatase; FBA: Frc-1,6-BP-aldolase; TPI: Triosephosphate isomerase; GAPDH: Glyceraldehyde-3P dehydrogenase; DHAP: Dihydroxyacetone phosphate

529 Interestingly, our phylogenetic analysis revealed the cd05800 subfamily as the most
530 primordial group of phosphoglucomutases. This group appears to be especially present in
531 bacterial classes that are considered deeply branching bacteria meaning they are relatively
532 close to the last common universal ancestor (LUCA). Examples for this are the classes of
533 Deinococci, Aquificae, Thermotogae, Bacteroidetes and Cyanobacteria, where this PGM
534 subfamily is widely distributed. This finding is supported by the fact that cd05800 members
535 can also be found in archaea. In agreement with this, the first characterized representative of
536 this group, Slr1334 shows both PGM and Glc-1,6-BP activity. This suggests that in primordial
537 systems these PGMs with broad functionality could have performed PGM reactions without
538 the requirement for specific Glc-1,6-BP synthase enzymes. During subsequent functional
539 diversification, the PGMs may have adopted unique functions, with specialization towards
540 efficient conversion of Glc-6-P into Glc-1P on the one hand, and more specialized formation
541 of the activating compound Glc-1,6-BP on the other hand. This assumption agrees with the
542 observation that many bacteria that have a cd05800 family member also possess a specialized
543 PGM of the cd05801 or cd03085 subfamily for efficient Glc-6P – Glc-1P conversion. This
544 includes the ensemble of all cyanobacteria. Conversely, many pathogenic bacteria that have
545 a PGM of the cd03089 type lack a cd5800 representative (**Table S4**) which raises the question
546 how those strains produce Glc-1,6-BP. To clarify these issues further investigations on αPHM
547 members from various bacterial groups are required.
548 We were able to show that the cd05800 PGM from the human gut commensal bacterium *B.*
549 *salyersiae* also catalyzes the synthesis of Glc-1,6-BP out of Frc-1,6-BP like Slr1334 (**Fig. 7**). In
550 the case of *B. salyersiae*, the enzyme appears to have an even higher catalytic efficiency for
551 the Glc-1,6-BP synthase reaction than for the standard PGM reaction (**Fig. S1**). Therefore, we
552 conclude that the formation of Glc-1,6-BP is a general feature of this group of PGMs.
553 Interestingly, members of the cd05800 group are also present in emerging human pathogenic
554 species like *Vibrio, Eggerthella* and *Brachyospyra* (**Fig. 1**) and are likely to play a key role in the
555 metabolism of these pathogens. In fact, due to their crucial role in capsule and cell wall
556 synthesis PGMs have been suggested as novel targets for the development of antiinfectives in
557 prophylactic and therapeutic interventions [5, 28]. It is tempting to speculate that Glc-1,6-BP
558 synthases of the cd05800 family, in virtue of their absence in eukaryotes, may also be
559 interesting candidates for the development of novel drugs modulating the microbiota with
560 little collateral damage to the host.

561 # Methods

562

563 **Isothermal, Single-Reaction DNA Assembly (Gibson Cloning)**

564 Cloning was performed as described by Gibson, Young [29] using *E. coli* NEB10β cells (details in
565 **Table S5**). All primers and plasmids used are shown in **Table S3** and **Table S4**, respectively.

566

567 **Cultivation of *Escherichia coli***

568 If not otherwise stated *E. coli* was grown in Luria-Bertani medium at 37°C [30]. For growth on
569 plates, 1.5% (w/v) agar-agar was added. For cells containing plasmids, the appropriate
570 concentration of antibiotics was used. All *E. coli* strains used in this study are listed in **Table**
571 **S5.**

572

573 **Protein overexpression and purification**

574 The plasmids used for protein overexpression are shown in **Table S4.** *Escherichia coli* Rosetta-
575 gami (DE3) (details **Table S5**) was used for the overexpression of all proteins. For this, cells
576 were cultivated in 2xYT (3.5% tryptone, 2% yeast extract, 0.5% NaCl; 1L of culture in 5L flasks)
577 at 37 °C until reaching exponential growth (OD_{600} 0.6-0.8). Protein overexpression was
578 induced by adding 75 µg/L anhydrotetracycline, followed by incubation at 20°C for 16 h. Cells
579 were harvested by centrifugation at 4000 g for 10 min at 4 °C. Cell disruption was performed
580 by sonication in 40 mL of lysis buffer (100 mM Tris-HCl pH 7.5, 500 mM NaCl, 10 mM $MgCl_2$,
581 20 mM Imidazole for His-tagged proteins and 100 mM Tris-HCl pH 8, 150 mM NaCl, 10 mM
582 $MgCl_2$ for Strep-tagged proteins) Lysis buffers were supplemented with DNAse I, and
583 cOmplete™ protease inhibitor cocktail (Roche, Basel)). The cell lysate was centrifuged at
584 40,000 g for 45 min at 4°C and the supernatant was filtered with a 0.22 µM filter.
585 For the purification of His-tagged proteins, 5 mL Ni-NTA HisTrap columns (GE Healthcare,
586 Illinois, USA) were used. The cell extracts were loaded onto the columns, washed with wash
587 buffer (50 mM Tris-HCl pH 7.4, 500 mM NaCl, and 50 mM Imidazole) and eluted with elution
588 buffer (50 mM Tris-HCl pH 7.4, 500 mm NaCl, and 500 mM Imidazole).

589

590

591 **Measurement of PGM activity of Sll0726 and Slr1334 in vitro**

592 Buffer for enzymatic reactions was composed of 50 mM HEPES-KOH pH 7.5, 150 mM KCl, 10
593 mM $MgCl_2$, 1 mM $NADP^+$, 1 mM DTT and 1 U/mL G6PDH from *Saccharomyces cerevisiae*
594 (G6378, Sigma Aldrich). For Sll0726 activity, 60 ng of Strep-tagged purified protein was added
595 to each reaction. For slr1334 activity, 650 ng of purified protein was added. For tests with
596 saturating Glc-1,6-BP concentrations, 60 µM Glc-1,6-BP have been used. Reaction was started
597 by the addition of glucose-1P. Reactions were carried out in a total of 300 µl in a 96-well
598 microplate. Absorption change at 340 nm was continuously measured for 15 min at 30 °C in a
599 TECAN Spark® Multiplate reader (Tecan Group AG, Männedorf, Switzerland). At least three
600 replicates were measured.
601
602 **Measurement of Glc-1,6-BP formation**

603 The reaction buffer was composed of 50 mM HEPES-KOH pH 7.5, 150 mM KCl and 10 mM
604 $MgCl_2$. To test the formation of Glc-1,6-BP out of Frc-1,6-BP 1 mM Frc-1,6-BP, 1 mM Glc1P or
605 1 mM Glc-6P were added in different combinations. To test the formation of Glc-1,6-BP out of
606 1,3-BPG instead of Frc-1,6-BP, 1 mM of ATP, 1 mM 3-PG and 60 µg PGK have been used.
607 Sll0726 and Slr1334 concentration were 30 µg/ml. The reactions were performed for 1.5 h at
608 30 °C followed by heat inactivation at 90°C for 10 minutes with subsequent centrifugation at
609 25000 g for 10 minutes at 4° C. The supernatants of the various reactions were used at 1:10
610 dilution in the Sll0726 activity assay.
611
612 **Frc-1,6-BP aldolase assay**

613 To measure the formation of Frc-1,6-BP by Slr1334, the reaction buffer was composed of 50
614 mM HEPES-KOH pH 7.5, 150 mM KCl, 10 mM $MgCl_2$, 0.2 mM NAD, 7 µg Slr1334, 1U/ml aldolase
615 from rabbit muscle and 1U/ml GDH from rabbit muscle. Concentrations of Glc-1,6-BP and Frc-
616 6P were varying depending on the experiment. Reaction was started by the addition of Glc-
617 1,6-BP or Frc-6P depending on the experiment.
618 To measure residual Frc-1,6-BP after running the Slr1334 reaction, the buffer was composed
619 of 50 mM HEPES-KOH pH 7.5, 150 mM KCl, 10 mM $MgCl_2$, 0.2 mM NAD, 0.02U/ml aldolase
620 from rabbit muscle and 1U/ml GDH from rabbit muscle.

621 All reactions were carried out in a total of 300 µl in a 96-well microplate Absorption change at
622 340 nm was continuously measured for 15 min at 30 °C in a TECAN Spark® Multiplate reader
623 (Tecan Group AG, Männedorf, Switzerland). The enzymatic activity was then calculated. At
624 least three replicates were measured.
625
626 **LC-MS measurement**

627 Sample preparation:
628 Reaction buffer was composed of 50 mM HEPES-KOH pH 7.5, 150 mM KCl and 10 mM $MgCl_2$.
629 For the reaction without enzyme 500 µM Frc-1,6-BP and 1 mM Glc1-P were added. For the
630 Slr1334 reaction 30 µg of Slr1334 have been used additionally. Reaction was carried out in a
631 total volume of 1 ml at 30 °C for 1h. Afterwards reaction was stopped by heat inactivation at
632 90° C followed by centrifugation at 25000 g for 10 minutes at 4°C.
633 For degradation of Frc-1,6-BP 1 mM NADH, 2U/ml of aldolase from rabbit muscle and 2U/ml
634 of GDH from rabbit muscle were added. Reaction was carried out followed by inactivation at
635 the same conditions as before.
636 LC/MS analysis:
637 LC/MS analysis was performed using an electrospray ionization time of flight (ESI-TOF) mass
638 spectrometer (MicrOTOF II; Bruker Daltonics), operated in negative ion-mode connected to
639 an UltiMate 3000 high-performance liquid chromatography (HPLC) system (Dionex). The
640 separation in the HPLC was carried out using a SeQuant ZIC-pHILIC column (PEEK 150 × 2.1
641 mm, 5 µm, 110 Å, Merck) at 30°C with an CH_3CN (buffer A) and 100 mM $(NH_4)_2CO_3$, pH 9
642 (buffer B) buffer system. A single run (injection volume of 5 µl) was performed with a flow rate
643 of 0.2 ml/min and a linear gradient of 25 min, reducing the concentration of buffer A from 82
644 to 42 %. Before (5 min) and after (10 min) the gradient, the column was equilibrated with 82 %
645 buffer A.
646
647 **Phylogenetic analysis of αPHM subfamilies**

648 The occurrence of members of the αPHM subfamilies was investigated in organisms included
649 in the NCBI RefSeq_protein database. Phylogenetic tree data were created using the ClustalW
650 implementation from the European Bioinformatics Institute (EMBL-EBI) and the phylogenetic
651 tree was created using the Interactive Tree Of Life (iTOL) v5 online tool [31, 32].

Statistical analysis

Statistical details for each experiment can be found in the figure legends. GraphPad PRISM was used to perform one-sided ANOVA to determine the statistical significance. Asterisks (*) in the figures symbolize the p-value: One asterisk represents $p \leq 0.05$, two asterisks $p \leq 0.01$, three asterisks $p \leq 0.001$, and four asterisks $p \leq 0.0001$

Acknowledgements

We thank Libera Lo Presti for her assistance in writing this manuscript and Gaia Bianchi for support in performing enzymatic assays.

This work was supported by FOR2816 “The Autotrophy-Heterotrophy Switch in Cyanobacteria: Coherent Decision-Making at Multiple Regulatory Layers” and EXC2121 “Controlling Microbes to Fight Infections (CMFI).

Author contributions

N.N. performed cloning, protein purification, enzymatic assays phylogenetic analysis and wrote manuscript. S.F. performed LC/MS analysis. K.F. conceived study, interpreted data and edited manuscript.

Competing interests

The authors declare no competing interest.

682 # References

683

684 1. Shackelford, G.S., C.A. Regni, and L.J. Beamer, *Evolutionary trace analysis of the α-D-*
685 *phosphohexomutase superfamily.* Protein Science, 2004. **13**(8): p. 2130-2138.

686 2. Stiers, K.M., A.G. Muenks, and L.J. Beamer, *Biology, Mechanism, and Structure of*
687 *Enzymes in the α-d-Phosphohexomutase Superfamily.* Advances in protein chemistry
688 and structural biology, 2017. **109**: p. 265-304.

689 3. Maliekal, P., et al., *Molecular identification of mammalian phosphopentomutase and*
690 *glucose-1,6-bisphosphate synthase, two members of the alpha-D-*
691 *phosphohexomutase family.* J Biol Chem, 2007. **282**(44): p. 31844-51.

692 4. Lu, S., et al., *CDD/SPARCLE: the conserved domain database in 2020.* Nucleic Acids
693 Res, 2020. **48**(D1): p. D265-d268.

694 5. Regni, C., P.A. Tipton, and L.J. Beamer, *Crystal structure of PMM/PGM: an enzyme in*
695 *the biosynthetic pathway of P. aeruginosa virulence factors.* Structure, 2002. **10**(2): p.
696 269-79.

697 6. Regni, C., et al., *Structural basis of diverse substrate recognition by the enzyme*
698 *PMM/PGM from P. aeruginosa.* Structure, 2004. **12**(1): p. 55-63.

699 7. Akutsu, J.-i., et al., *Characterization of a Thermostable Enzyme with*
700 *Phosphomannomutase/Phosphoglucomutase Activities from the Hyperthermophilic*
701 *Archaeon Pyrococcus horikoshii OT3.* The Journal of Biochemistry, 2005. **138**(2): p.
702 159-166.

703 8. Liu, Y., W.J. Ray, Jr., and S. Baranidharan, *Structure of rabbit muscle*
704 *phosphoglucomutase refined at 2.4 A resolution.* Acta Crystallogr D Biol Crystallogr,
705 1997. **53**(Pt 4): p. 392-405.

706 9. Backe, P.H., et al., *Structural basis for substrate and product recognition in human*
707 *phosphoglucomutase-1 (PGM1) isoform 2, a member of the α-d-phosphohexomutase*
708 *superfamily.* Scientific Reports, 2020. **10**(1): p. 5656.

709 10. Leloir, L.F., R.E. Trucco, and et al., *The co-enzyme of phosphoglucomutase.* Arch
710 Biochem, 1948. **19**(2): p. 339.

711 11. Naught, L.E. and P.A. Tipton, *Kinetic Mechanism and pH Dependence of the Kinetic*
712 *Parameters of Pseudomonas aeruginosa*
713 *Phosphomannomutase/Phosphoglucomutase.* Archives of Biochemistry and
714 Biophysics, 2001. **396**(1): p. 111-118.

715 12. Carreras, J., et al., *Bisphosphorylated metabolites of glycerate, glucose, and fructose:*
716 *Functions, metabolism and molecular pathology.* Clinical Biochemistry, 1986. **19**(6): p.
717 348-358.

718 13. Joshi, J.G. and P. Handler, *PHOSPHOGLUCOMUTASE. I. PURIFICATION AND*
719 *PROPERTIES OF PHOSPHOGLUCOMUTASE FROM ESCHERICHIA COLI.* J Biol Chem,
720 1964. **239**: p. 2741-51.

721 14. Lindahl, M. and F.J. Florencio, *Thioredoxin-linked processes in cyanobacteria are as*
722 *numerous as in chloroplasts, but targets are different.* Proceedings of the National
723 Academy of Sciences, 2003. **100**(26): p. 16107-16112.

724 15. Mehra-Chaudhary, R., et al., *Crystal structure of a bacterial phosphoglucomutase, an*
725 *enzyme involved in the virulence of multiple human pathogens.* Proteins, 2011. **79**(4):
726 p. 1215-1229.

727 16. Doello, S., et al., *Regulatory phosphorylation site tunes Phosphoglucomutase 1 as a*
728 *metabolic valve to control mobilization of glycogen stores.* bioRxiv, 2021: p.
729 2021.04.15.439997.

730 17. Lian Liu, H.H., Hong Gao, and Xudong Xu, *Role of two phosphohexomutase genes in*
731 *glycogen synthesis in Synechocystis sp. PCC6803.* Chinese Science Bulletin, 2013.
732 **58**(36).

733 18. Maino, V.C. and F.E. Young, *Regulation of Glucosylation of Teichoic Acid: II. PARTIAL*
734 *CHARACTERIZATION OF PHOSPHOGLUCOMUTASE IN BACILLUS SUBTILIS 168.* Journal
735 of Biological Chemistry, 1974. **249**(16): p. 5176-5181.

736 19. Fazi, A., et al., *Purification and partial characterization of the phosphoglucomutase*
737 *isozymes from human placenta.* Prep Biochem, 1990. **20**(3-4): p. 219-40.

738 20. Naught, L.E. and P.A. Tipton, *Formation and reorientation of glucose 1,6-*
739 *bisphosphate in the PMM/PGM reaction: transient-state kinetic studies.*
740 Biochemistry, 2005. **44**(18): p. 6831-6.

741 21. Ray, W.J., Jr. and G.A. Roscelli, *A KINETIC STUDY OF THE PHOSPHOGLUCOMUTASE*
742 *PATHWAY.* J Biol Chem, 1964. **239**: p. 1228-36.

743 22. Jolly, L., et al., *Autophosphorylation of Phosphoglucosamine Mutase from*
744 *Escherichia coli.* Journal of Bacteriology, 2000. **182**(5): p. 1280-1285.

745 23. Morava, E., et al., *Impaired glucose-1,6-biphosphate production due to bi-allelic*
746 *PGM2L1 mutations is associated with a neurodevelopmental disorder.* Am J Hum
747 Genet, 2021. **108**(6): p. 1151-1160.

748 24. Leloir, L.F., R.E. Trucco, and et al., *The formation of glucose diphosphate by*
749 *Escherichia coli.* Arch Biochem, 1949. **24**(1): p. 65-74.

750 25. Veiga-da-Cunha, M., et al., *Mammalian phosphomannomutase PMM1 is the brain*
751 *IMP-sensitive glucose-1,6-bisphosphatase.* The Journal of biological chemistry, 2008.
752 **283**(49): p. 33988-33993.

753 26. Maino, V.C. and F.E. Young, *Regulation of glucosylation of teichoic acid. II. Partial*
754 *characterization of phosphoglucomutase in Bacillus subtilis 168.* J Biol Chem, 1974.
755 **249**(16): p. 5176-81.

756 27. Waygood, E.B., J.S. Mort, and B.D. Sanwal, *The control of pyruvate kinase of*
757 *Escherichia coli. Binding of substrate and allosteric effectors to the enzyme activated*
758 *by fructose 1,6-bisphosphate.* Biochemistry, 1976. **15**(2): p. 277-282.

759 28. Zhang, Y., et al., *The Brucella melitensis M5-90 phosphoglucomutase (PGM) mutant is*
760 *attenuated and confers protection against wild-type challenge in BALB/c mice.* World
761 Journal of Microbiology and Biotechnology, 2016. **32**(4): p. 58.

762 29. Gibson, D.G., et al., *Enzymatic assembly of DNA molecules up to several hundred*
763 *kilobases.* Nature Methods, 2009. **6**(5): p. 343-345.

764 30. Bertani, G., *Studies on lysogenesis. I. The mode of phage liberation by lysogenic*
765 *Escherichia coli.* J Bacteriol, 1951. **62**(3): p. 293-300.

766 31. Letunic, I. and P. Bork, *Interactive Tree Of Life (iTOL) v5: an online tool for*
767 *phylogenetic tree display and annotation.* Nucleic Acids Research, 2021. **49**(W1): p.
768 W293-W296.

769 32. Madeira, F., et al., *The EMBL-EBI search and sequence analysis tools APIs in 2019.*
770 Nucleic acids research, 2019. **47**(W1): p. W636-W641.
771

Figure Legends

Figure 1: **Phylogenetic tree of the αPHM subfamilies that are considered to be "PGM-like" according to CDD**

The tree was built on the taxonomy based on the protein sequences present in the NCBI RefSeq_protein database. The CDD subfamilies cd03086, cd03088, cd05802 and cd05805, which are known to catalyze distinct reactions, were omitted from the analysis. The organisms investigated in this study are highlighted in bold letters.

Figure 2: Slr1334 shows lower PGM activity then Sll0726 and behaves differently in presence of Frc-1,6-BP

Shown are the Michaelis-Menten kinetics of Sll0726 (A) and Slr1334 (B): in black, without addition of effectors; in light grey in the presence of 60 µM Glc-1,6-BP; in blue, in the presence of 100 µM Frc-1,6-BP. Three replicates were measured for each data-point. Error bars represent the SD.

Figure 3: Slr1334 produces a compound out of Frc-1,6-BP that strongly activates Sll0726

Shown is the Sll0726 activity: in dark grey, at different Glc-1,6-BP concentrations; in blue, after addition of the supernatant of the Slr1334 reaction; in light grey, after addition of the supernatant of the Sll0726 reaction as a control; in white, after addition of the sole phosphosugars without enzyme as further control. The different combinations of substrates used for the Slr1334 reaction and controls are indicated on the X-axis. Values represent relative activity compared to the Sll0726 reaction with 0 µM Glc-1,6-BP, which was considered 100%. Three biological replicates were measured for each datapoint. Error bars represent the SD; asterisks represent the statistical significance

Figure 4: LC-MS analysis reveals that Slr1334 metabolizes Frc-1,6-BP into a molecule of identical mass that is not degraded by Frc-1,6-BP-aldolase

Analysis of the products of the reaction without (A) and with Slr1334 (B) via LC/MS. Shown are the base peak chromatograms (BPC) in the mass range $(M-H)^-$ m/z = 79–1,601 (grey) and the extracted ion chromatograms (EIC) based on the exact masses of NAD+ $(M-H)^-$= 662.101 m/z (light blue), NADH $(M-H)^-$= 664.117 m/z (red), Glycerol 3-P $(M-H)^-$= 171.006 m/z (yellow), Glc-1,6-BP/Frc-1,6-BP $(M-H)^-$= 338.988 m/z (purple). The presence of the NAD+ (blue) and Glycerol-3P (yellow) peaks in (B) shows that Frc-1,6-BP was not fully metabolized into Glc-1,6-BP. Magnification and adjustment of the graphs in (A) and (B) is clear evidence of the absence (C) or formation (D) of Glc-1,6-BP.

813 **Figure 5: Slr1334 produces Glc-1,6-BP out of Frc-1,6-BP in an equilibrium reaction**

814 Shown is the Frc-1,6-BP-aldolase activity: in dark blue, after addition of the supernatant of
815 the Slr1334 reaction; in light blue, after addition of the supernatant of the Sll0726 reaction as
816 a control; in black, after addition of the supernatant without any enzyme. In dark grey and
817 light grey, the aldolase activity measured at Frc-1,6-BP concentrations of 25 µM and 50 µM,
818 respectively, as further control.
819 Frc-1,6-BP was used at concentrations of 500 µM in the Slr1334 reaction and respective
820 control reactions. Therefore, its final concentration in the Sll0726 assay after 1:10 dilution was
821 expected to be 50 µM assuming no consumption of Frc-1,6-BP in the Slr1334 reaction. Three
822 replicates were measured for each datapoint. Error bars represent the SD.
823

824 **Figure 6: Slr1334 catalyzes the reverse reaction to form Frc-1,6-BP out of Glc-1,6-BP and Frc-**
825 **6P**

826 (A) Activity of Slr1334 (blue), Sll0726 (grey), and rabbit PGM1 (black) using 50 µM Glc-1,6-BP
827 and 5 mM Frc-6P. (B) Michaelis-Menten kinetics of Slr1334 using different concentrations of
828 Frc-6P and 50 µM Glc-1,6-BP. (C) Slr1334 reaction at different concentrations of Glc-1,6-BP
829 and 0.5 mM Frc-6P. Three replicates were measured for each datapoint. Error bars represent
830 the SD; asterisks represent the statistical significance.
831

832 **Figure 7: Slr1334 homologue from *B.salyersiae* also forms Glc-1,6-BP out of Frc-1,6-BP**

833 Shown is the activity of Sll0726: blue, after addition of the supernatant of the *B. salyersiae*
834 PGM reaction; in light grey, after addition of the supernatant of the Slr1334 reaction as a
835 positive control; in dark grey, without any effectors as a negative control. The different
836 combinations of substrates used for the *B. salyersiae* PGM and Slr1334 control reaction are
837 indicated on the X-axis. Values represent relative activity compared to the Sll0726 reaction
838 without any effectors, which was considered 100%. Error bars represent the SD; asterisks
839 represent the statistical significance.

840

841 **Figure 8: Potential role of Slr1334 in glycolysis**

842 Shown is the potential role of Slr1334 in regulating activity of αPHMs and the concentration
843 of key metabolites in glycolysis. PGM: Phosphoglucomutase; PGI: Glc-6P-Isomerase; PFK:
844 Phosphofruktokinase; FBAse: Fructose-6P phosphatase; FBA: Frc-1,6-BP-aldolase; TPI:
845 Triosephosphate isomerase; GAPDH: Glyceraldehyde-3P dehydrogenase; DHAP:
846 Dihydroxyacetone phosphate
847